A MODIFIED ALGORITHM FOR A LOUDSPEAKER LINE ARRAY MULTI-LOBE CONTROL

Stefania Cecchi, Valeria Bruschi

Dept. of Information Engineering
Università Politecnica delle Marche
Ancona, IT
s.cecchi@dii.univpm.it

Michele Frati, Marco Secondini, Andrea Tanoni

FBT Elettronica
Recanati, IT
michele.frati@fbt.it

ABSTRACT

The creation of personal sound zones is an effective solution for delivering personalized auditory experiences in shared spaces. Their applications span various domains, including in-car entertainment, home and office environments, and healthcare functions. This paper presents a novel approach for the creation of personal sound zones using a modified algorithm for multi-lobe control in loudspeaker line array. The proposed method integrates a pressure-matching beamforming algorithm with an innovative technique for reducing side lobes, enhancing the precision and isolation of sound zones. The system was evaluated through simulations and experimental tests conducted in a semi-anechoic environment and a large listening room. Results demonstrate the effectiveness of the method in creating two separate sound zones.

1. INTRODUCTION

Personal sound zones (PSZs) are innovative audio solutions that provide individualized auditory experiences within shared environments. Using advanced sound field manipulation and beamforming techniques, PSZs enable the creation of distinct areas where people can hear separate audio content without interference from neighboring zones [1]. They enhance in-car entertainment by allowing passengers to hear different content simultaneously [2, 3], improve privacy and productivity in home and office environments [4], and provide therapeutic and communication benefits in healthcare facilities [5]. The work presented in this paper aims to create two personal sound zones by applying a multi-lobe control algorithm to a loudspeaker line array.

Multizone audio reproduction is usually achieved using loudspeaker line arrays since they can focus sound toward specific zones, minimizing unwanted reflections or echoes. Each loudspeaker signal is properly modified to shape the acoustic field and direct the sound. The simplest approach is the delay and sum beamforming (DS) [6], which is based on the application of proper delays to the loudspeaker signals, so that the individual contributions recombine in phase at the center of the target zone. More accurate techniques are based on applying filters obtained through optimization processes. The literature presents a variety of techniques, each defined by the specific cost function employed in the optimization procedure. A widely adopted method is acoustic contrast control (ACC) [7], which focuses on optimizing acoustic contrast by maximizing the ratio of energy reproduced within the target sound field (bright zone) to the total energy emitted by the sound source. A variant solution to ACC is the energy difference maximization (EDM) [8], based on maximizing the difference between the energy in the bright zone and that in the dark zone, where sound pressure levels are minimized. A notable advantage of EDM is that it eliminates the need for matrix inversion, which is a requirement in ACC. Moreover, the EDM method allows for appropriately controlling the radiation efficiency in the bright zone, although the acoustic contrast resulting from this algorithm is generally lower than what would be achieved by applying the ACC [8]. Although ACC algorithms are widely used in the literature, additional methods have been developed based on the established theory of sound field synthesis (SFS) [9]. Among these, those centered on the technique called pressure matching (PM) stand out, where filters are designed in such a way as to minimize the error between the desired sound field and the one actually generated by the electro-acoustic system [10]. Generally, a least squares (LS) approach is used to minimize this type of error. Although this approach achieves improved planarity, which determines the resemblance of the sound field to a plane wave, it produces lower acoustic contrast compared to the ACC method [6]. Another technique based on SFS is the planarity control (PC) methods [11], designed to optimize acoustic planarity. These approaches achieve an acoustic contrast comparable to ACC while maintaining planarity similar to PM. In [12], another solution named least squares frequency invariant (LSFI) beamforming is presented and applied for the development of a multiband acoustic crosstalk canceler. This method is based on a convex optimization with constraints that minimizes the difference between the effective and the desired response. In [12], the LSFI beamforming is used to improve the performance of the recursive ambiophonic crosstalk elimination (RACE) algorithm by directing the sound towards the ears of the listener. In [13], the same system is implemented, comparing LSFI beamforming and PM algorithm. Objective and subjective tests have proven that pressure matching technique outperform the LSFI approach.

In this paper, the pressure matching algorithm is implemented and tested for the creation of two target sound zones, i.e., double beamforming. Moreover, this approach is combined with an algorithm for the reduction of the side lobes that is based on the application of a shading function depending on the frequency and the desired direction. The proposed system has been tested with a loudspeaker line array through simulations, in which synthetic impulse responses are considered, and real-world experiments. The real tests have been performed in a semi-anechoic chamber and a large listening room. Results have proven the effectiveness of the approach.

The paper is organized as follows. Section 2 describes the

pressure matching algorithm and the side lobes reduction technique. Section 3 shows the results obtained in the simulated scenario and the real-world scenario. Finally, Section 4 concludes the paper.

2. DESCRIPTION OF THE ALGORITHM

The proposed algorithm is based on the pressure matching algorithm that allows for obtaining the optimal filters that must be applied to direct the sound towards a target direction. The PM is combined with the application of a shading function for the side lobes reduction (SLR). The general scheme of the system is shown in Figure 1. The description of the two algorithms, which are applied jointly, follows.

2.1. Pressure Matching Algorithm

The pressure matching is an algorithm developed in [10]. As the name of the technique states, the PM aims at getting a reproduced sound field $\mathbf{p}$ that has to be the most similar to a desired one $\hat{\mathbf{p}}$. Consequently, the objective is to minimize a cost function J given by the sum of a squared norm error (first addendum) and a regularization term (second addendum), i.e.,

$$J = \|\hat{\mathbf{p}} - \mathbf{H}\mathbf{q}\|^2 + \beta\|\mathbf{q}\|^2, \tag{1}$$

where $\mathbf{H}$ is a matrix whose elements represent the electro-acoustical transfer functions relating each loudspeaker of the array to the positions in which the sound field needs to be controlled, $\mathbf{q}$ are the complex source strengths that drive the loudspeakers (i.e., the filters) and β is a regularization parameter. The optimal source strength vector $\mathbf{q}_{\text{opt}}$ that minimizes the cost function can be found by solving the eq. (1) in a least-squares sense:

$$\mathbf{q}_{\text{opt}} = \left[\mathbf{H}^H\mathbf{H} + \beta\mathbf{I}\right]^{-1}\mathbf{H}^H\hat{\mathbf{p}}, \tag{2}$$

where $\mathbf{I}$ is an identity matrix. The desired sound field $\hat{\mathbf{p}}$ is chosen following the guidelines presented in [10], and the electro-acoustical transfer functions are obtained in a simulated way or with real measurements. At this point, it is sufficient to solve the eq. (2) to find the optimal filters that need to be placed at the input of the array system. Considering an array of an odd number N of loudspeakers, the matrix $\mathbf{q}_{\text{opt}} = [\mathbf{q}_{-\frac{N-1}{2}}, ..., \mathbf{q}_m, ..., \mathbf{q}_{\frac{N-1}{2}}]$ contains the complex frequency domain filters. The respective time-domain filter of the mth loudspeaker $q_m(t)$ is obtained through an inverse FFT (IFFT), and the signal of the mth loudspeaker can be written as

$$s_m(t) = x(t) * q_m(t), \tag{3}$$

where $*$ expresses the convolution operation, and $x(t)$ is the input sound signal.

2.2. Side Lobes Reduction

The loudspeaker signal is modified by applying a shading factor obtained following the approach of [14]. This approach defines a family of optimal shading functions that aim to reduce the side lobes. The shaded loudspeaker signal is then obtained as

$$s_m^{shaded}(t) = \sigma_m \cdot s_m(t), \tag{4}$$

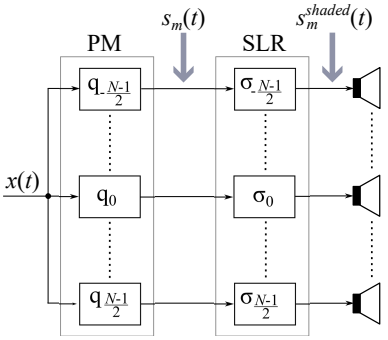

Figure 1: *Scheme of the proposed system, including the pressure matching (PM) algorithm and the side lobes reduction (SLR).*

where $s_m(t)$ is the signal of the mth loudspeaker obtained by eq. (3), and σ_m is the shading window, with length N, and calculates as follows:

$$\sigma_m = \begin{cases} \frac{\alpha}{\sinh\alpha} I_0\left[\alpha\sqrt{1-k\left(\frac{m}{N-1}\right)^2}\right], & \text{if } \alpha > 0, \\ 1, & \text{if } \alpha = 0. \end{cases} \tag{5}$$

In the first case with $\alpha > 0$ the shading function is described as the Kaiser window [15] defined in the range $-\frac{N-1}{2} \leq m \leq \frac{N-1}{2}$, and I_0 represents the modified Bessel function of the first kind. A coefficient $k = 0.01$ has been used as the best value that gave the best results after several tests. The parameter α depends on the frequency and is computed as

$$\alpha = \begin{cases} \pi\sqrt{(N-1)^2u_1^2 - 1}, & \text{if } (N-1)^2u_1^2 - 1 > 0, \\ 0, & \text{if } (N-1)^2u_1^2 - 1 \leq 0, \end{cases} \tag{6}$$

where u_1 is the normalized frequency at which the main lobe is half as wide, i.e.,

$$u_1 = f \cdot \frac{d}{c}(\sin\theta_1 - \sin\theta_0), \tag{7}$$

where f is the frequency, d is the loudspeaker distance, $c = 343$ m/s is the speed of sound, θ_0 is the direction of the main lobe, and θ_1 is the angle of the first zero of the main lobe.

3. EXPERIMENTAL RESULTS

The results are obtained through simulations and real-world experiments. In both cases, a linear array of 16 loudspeakers that has a distance of $d = 0.1$ m was taken into account. The performance of the system is estimated through directivity patterns evaluated in

Table 1: *Octave bands used for the experimental results.*

Band	f_l [Hz]	f_0 [Hz]	f_h [Hz]
#1	177	250	355
#2	355	500	710
#3	710	1000	1420
#4	1420	2000	2840
#5	2840	4000	5680
#6	5680	8000	11360

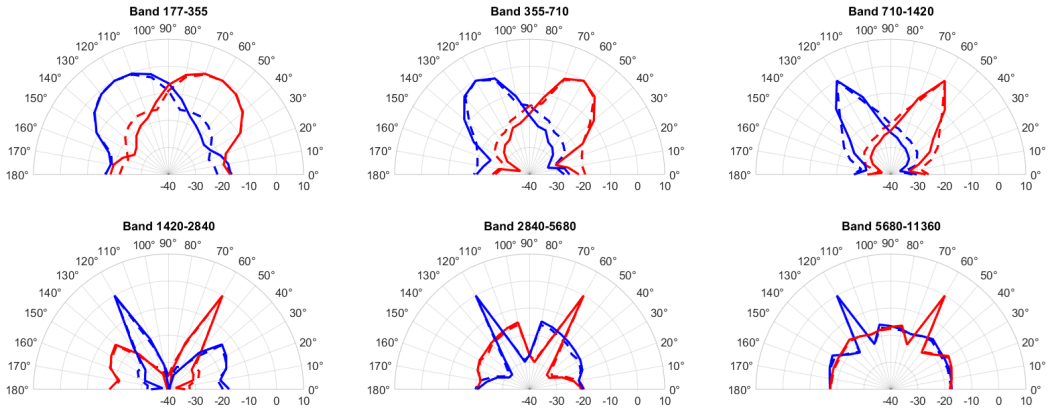

Figure 2: *Directivity patterns obtained with simulated IRs pointing at* 60° *(blue curve) and at* 120° *(red curve), before (dashed curve) and after applying the side lobes reduction (solid curve).*

six octave frequency bands, reported in Table 1. For each band, the cut-off frequencies f_l and f_h which define the limits, and the center frequency f_0 is described. In every frequency range $[f_l, f_h]$, the value of the directivity pattern $\mathcal{D}$ in dB is computed for each measurement position $\mathbf{x}_m$ as

$$\mathcal{D}(\mathbf{x}_m) = 10\log_{10}\left(\frac{\frac{1}{f_h - f_l}\int_{f_l}^{f_h} |\mathbf{p}(\mathbf{x}_m, f)|^2\, df}{p^2_{\text{MAX}}}\right), \quad (8)$$

where p^2_{MAX} is defined as:

$$p^2_{\text{MAX}} = \left(\max_m \frac{1}{f_h - f_l}\int_{f_l}^{f_h} |\mathbf{p}(\mathbf{x}_m, f)|^2\, df\right), \quad (9)$$

and the $\mathbf{p}(\mathbf{x}_m, f)$ is the value of the sound pressure at the point $\mathbf{x}_m$ for the frequency f, obtained after the application of the beamforming filters.

3.1. Simulated scenario

The algorithm was first evaluated through Matlab simulations, considering synthetic impulse responses obtained using the "Room Impulse Response (RIR) Generator" tool [16]. Figure 2 shows the results obtained by the pressure matching algorithm considering two directions, i.e., 60° (in blue) and 120° (in red). The result of the PM algorithm is shown with the dashed line, while the result obtained after the side lobes reduction is shown with the solid lines. From the figure, it can be seen that the sound is focused towards the desired directions, and it is more directive as the frequency increases. However, from the fourth band and above, the side lobes increase their width. This phenomenon is due to the spatial aliasing that occurs for frequencies higher than f_{SA}, computed as

$$f_{\text{SA}} = \frac{c}{d\big(1 + |\sin\theta|\big)}, \quad (10)$$

where $c = 343$ m/s, $d = 0.1$ is the loudspeaker distance, and θ is the pointing angle. Referring to Figure 2, where $\theta = 60^\circ$ and $\theta = 120^\circ$, $f_{\text{SA}} = 1.82$ kHz, which is contained in the fourth band.

The effect of the shading function is not so evident and is mostly focused on the low and middle frequencies, where the side lobes are reduced. In the first two bands, the directivity patterns are more homogeneous. The best result is obtained in the third band, where the sound is more directive. Differently, at higher frequencies, the shading does not significantly change the polar patterns.

3.2. Real scenario: Semi-anechoic chamber

The first real-world experiment was carried out in a semi-anechoic chamber. The setup scheme used for the experiments is shown in Figure 3(a). The PC is connected to the MOTU 24 I/O sound card that manages the line array composed of 16 loudspeakers, and the pre-amplifier Presonus D-8 connected to the Behringer B-5 microphone, placed at a distance of 3 meters from the line array. The impulse responses were measured using the exponential sweep with a sampling frequency of 48 kHz using the Nu-Tech software [17]. A photo of the measurement procedure is reported in Figure 4(a). Figure 5 shows the directivity patterns obtained with the IRs measured in the semi-anechoic chamber. The experiment considers the double beamforming at 60° and 120°. The application of real impulse responses makes the spatial aliasing phenomenon more evident, especially above 3 kHz. Although this increment of the side lobes, the sound pressure level in correspondence with the target direction is always at least 10 dB greater than the maximum of the secondary lobes. The application of the side lobes reduction modifies the directivity plots in the low frequencies, especially in the second band, where the sound is more directive. However, the improvement is not so noticeable. The results are in line with the ones obtained in the simulations, confirming the effectiveness of the algorithm.

3.3. Real scenario: Large room

The second real-world experiment was carried out in a large listening room, using the setup shown in Figure 3(b). The sound card and the loudspeaker array are the same used in the semi-anechoic chamber and presented in Section 3.2. Differently, the microphone was a Brüel & Kjær - Type 4191, which needs a power supply, and the pre-amplifier MIDAS XL42 2 Channels was adopted. The distance between the microphone and the array was 3.5 m. The same sampling frequency and software of Section 3.2 were used for the IRs measurement. A photo of the measurement procedure is reported in Figure 4(b). Figure 6 shows the directivity patterns

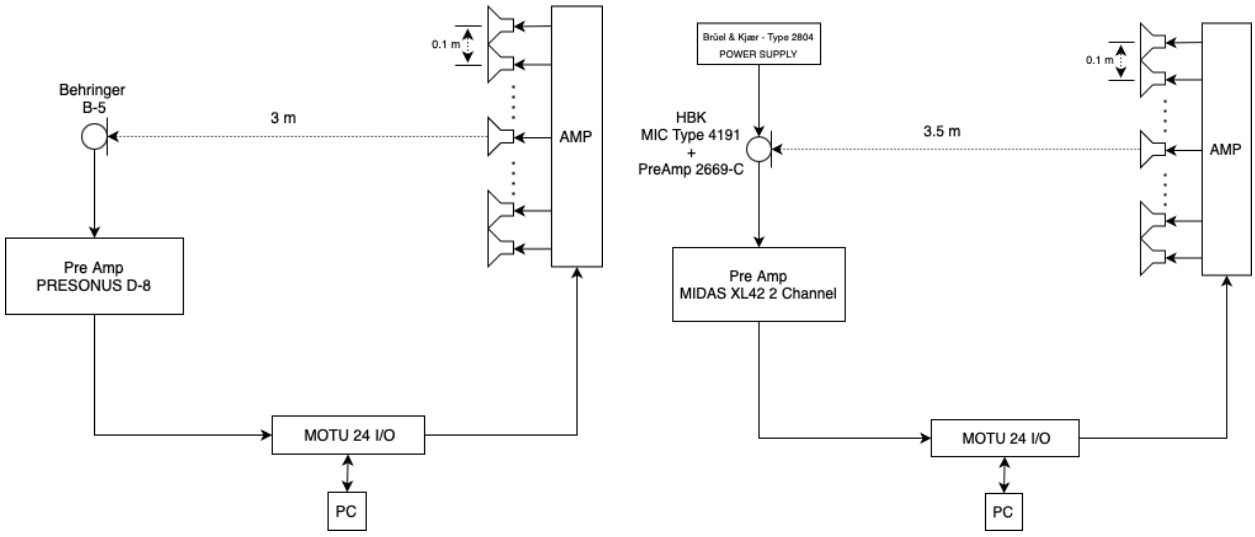

Figure 3: *Measurement setup (a) in the semi-anechoic chamber, and (b) in the large listening room.*

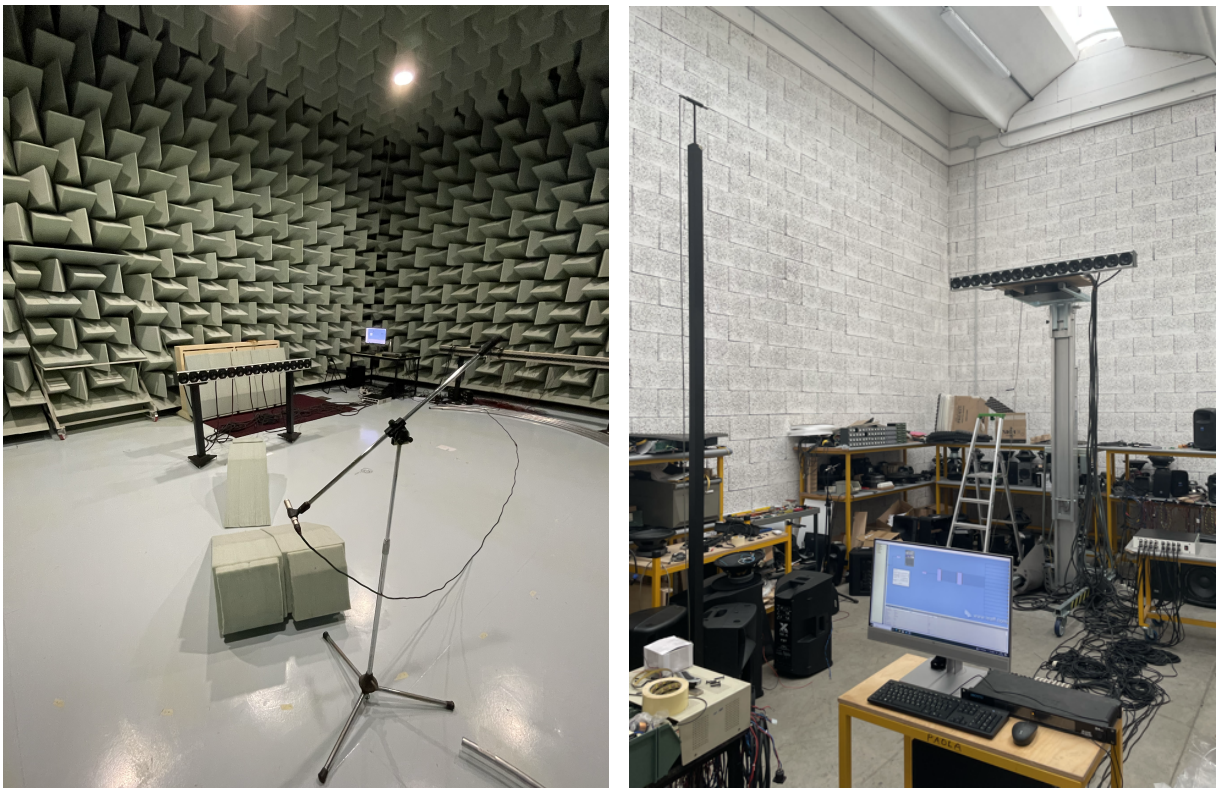

(a) (b)

Figure 4: *Photo of the measures taken (a) in the semi-anechoic chamber, and (b) in the large listening room.*

obtained with the IRs measured in the listening room. Also in this case, the double beamforming is applied pointing at 60° and 120°. The directivity is better for high frequencies above 700 Hz. With the increase of the frequency, the secondary lobes rise. The spatial aliasing is more evident than in the semi-anechoic chamber, due to the numerous reflections of the room. In this case, the application of the side lobes reduction is extremely evident in all the frequency bands. The sound pressure level of the main lobe is always at least

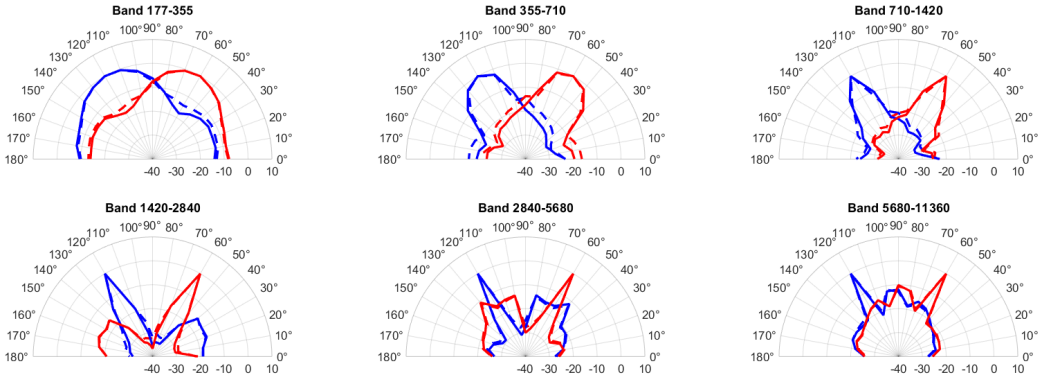

Figure 5: *Directivity patterns obtained with IRs measured in the semi-anechoic chamber pointing at* 60° *(blue curve) and at* 120° *(red curve), before (dashed curve) and after applying the side lobes reduction (solid curve).*

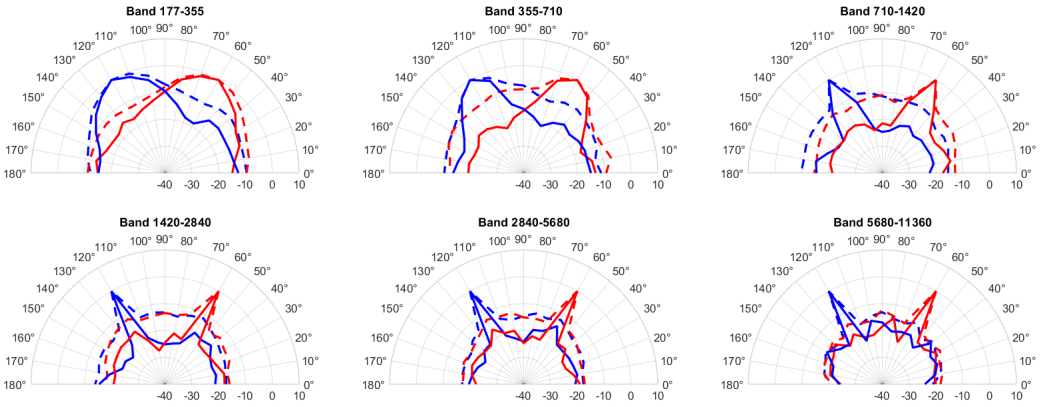

Figure 6: *Directivity patterns obtained with IRs measured in the large room pointing at* 60° *(blue curve) and at* 120° *(red curve), before (dashed curve) and after applying the side lobes reduction (solid curve).*

5 dB greater than the maximum of the secondary lobes before the application of the shading function. After the reduction of the side lobes, the difference between the main lobe and the maximum of the secondary lobes is increased to 10 dB, as obtained in the simulations and in the semi-anechoic chamber.

4. CONCLUSIONS

The paper has presented an algorithm for the multi-lobe control of a loudspeaker line array. The system uses the pressure-matching beamforming algorithm, based on the minimization procedure with regularization. Moreover, a shading function for the side lobes reduction is applied to improve the directivity of the sound. The algorithm has been tested in a simulated scenario and two real-world environments, i.e., a semi-anechoic chamber and a large listening room. In the experiments, personal sound zones were created by designing two distinct beamforming patterns, each with a single main lobe directed toward a different target location. The algorithm has demonstrated strong performance, enhancing directivity at higher frequencies. Moreover, the impact of reducing side lobes has been assessed. In both the simulated scenario and the semi-anechoic chamber, this reduction has led to a modest improvement in directivity patterns at lower frequencies, specifically up to 1.5 kHz. In the large listening room, the reflective nature of the environment makes the spatial aliasing of beamforming more pronounced. Nevertheless, applying the side lobes reduction in the large room has resulted in significant improvements across all frequencies.

Possible future developments to improve the performance of the proposed algorithm could include enhancing the accuracy of the function that determines the sound pressure at the bright points and improving the measurement procedure by increasing the resolution of the measurement points. Regarding the algorithm for reducing the side lobes, its performance at high frequencies can be improved to reduce annoying contributions caused by spatial aliasing phenomena.

5. REFERENCES

[1] W.F. Druyvesteyn and J. Garas, "Personal sound," *Journal of the Audio Engineering Society*, vol. 45, no. 9, pp. 685–701, 1997.

[2] A. Borroni, M. Martalò, A. Costalunga, C. Tripodi, and R. Raheli, "Pressure matching with optimized target phase for personal sound zone systems," in *International Conference on Electrical, Computer, Communications and Mechatronics Engineering (ICECCME)*. IEEE, 2022, pp. 1–6.

[3] J. Cheer, S. J. Elliott, and M. F. S. Gálvez, "Design and implementation of a car cabin personal audio system," *Journal of the Audio Engineering Society*, vol. 61, no. 6, pp. 412–424, 2013.

[4] T. Betlehem, W. Zhang, M. A. Poletti, and T. D. Abhayapala, "Personal sound zones: Delivering interface-free audio to multiple listeners," *IEEE Signal Processing Magazine*, vol. 32, no. 2, pp. 81–91, 2015.

[5] K. Fangel Skov, P. Axel Nielsen, and J. Kjeldskov, "Tuning shared hospital spaces: Sound zones in healthcare," in *Proceedings of the 18th International Audio Mostly Conference*, 2023, pp. 63–70.

[6] M. Olik, J. Francombe, P. Coleman, P. J. B. Jackson, M. Olsen, M. Møller, R. Mason, and S. Bech, "A comparative performance study of sound zoning methods in a reflective environment," in *Proc. of 52nd International Audio Engineering Society Conference*, Guildford, UK, Sep 2013.

[7] J. W. Choi and Y. H. Kim, "Generation of an acoustically bright zone with an illuminated region using multiple sources," *The Journal of the Acoustical Society of America*, vol. 111, no. 4, pp. 1695–1700, 2002.

[8] M. Shin, S. Q. Lee, F. M. Fazi, P. A. Nelson, D. Kim, S. Wang, K. H. Park, and J. Seo, "Maximization of acoustic energy difference between two spaces," *The Journal of the Acoustical Society of America*, vol. 128, no. 1, pp. 121–131, 2010.

[9] J. Ahrens, *Analytic methods of sound field synthesis*, Springer Science & Business Media, 2012.

[10] F. Olivieri, M. Shin, F. M. Fazi, P. A. Nelson, and P. Otto, "Loudspeaker array processing for multi-zone audio reproduction based on analytical and measured electroacoustical transfer functions," in *Proc. of 52nd International Audio Engineering Society Conference*, Guildford, UK, Sep 2013.

[11] P. Coleman, P. Jackson, M. Olik, and J. A. Pedersen, "Optimizing the planarity of sound zones," in *Proc. of 52nd International Audio Engineering Society Conference*, Guildford, UK, Sep 2013.

[12] C. Hohnerlein and J. Ahrens, "Perceptual evaluation of a multiband acoustic crosstalk canceler using a linear loudspeaker array," in *2017 IEEE International Conference on Acoustics, Speech and Signal Processing (ICASSP)*. IEEE, 2017, pp. 96–100.

[13] V. Bruschi, N. Ortolani, S. Cecchi, and F. Piazza, "Immersive sound reproduction in real environments using a linear loudspeaker array," in *Proc. 147th Audio Engineering Society Convention*. Audio Engineering Society, 2019.

[14] R. Schmidmaier and D. G. Meyer, "Dynamic amplitude shading of electronically steered line source arrays," in *Audio Engineering Society Convention 92*. Audio Engineering Society, 1992.

[15] J. Kaiser and R. Schafer, "On the use of the I0-sinh window for spectrum analysis," *IEEE Transactions on Acoustics, Speech, and Signal Processing*, vol. 28, no. 1, pp. 105–107, 1980.

[16] E. Habets, "Room impulse response generator," *Internal Report*, pp. 1–17, 01 2006.

[17] A. Lattanzi, F. Bettarelli, and S. Cecchi, "Nu-tech: The entry tool of the hartes toolchain for algorithms design," in *Proc. 124th Audio Engineering Society Convention*, Amsterdam, The Netherlands, May 2008, pp. 1–8.